

EPR Studies of Photoreduction of Ni/TiO₂ Catalysts

Shu-Hua Chien* (簡淑華), Yu-Wen Wei (魏易文) and Mau-Chen Lin (林茂成)
 Institute of Chemistry, Academia Sinica, Taipei 11529, and Department of Chemistry,
 National Taiwan University, Taipei 10664, Taiwan, R.O.C.

Irradiations of Ni/TiO₂ catalyst by UV in hydrogen at 77 K produced not only Ni⁺ ions on the catalyst surface, but also Ni³⁺ and Ti³⁺ species in bulk or near the interface between nickel and titania. These photo-generated species were detected and characterized by low temperature electron paramagnetic resonance (EPR) spectroscopy. Relative spin concentrations of the photogenerated paramagnetic species (Niⁿ⁺ and Ti³⁺) varied with the nickel content in titania. A high nickel content in the sample resulted in a high peak intensity ratio of Niⁿ⁺ to Ti³⁺. It was found that the photoinduced self-redox reaction of Ni²⁺ ions to form Ni⁺ and Ni³⁺ ions has a priority over the photoreduction of Ti⁴⁺ to Ti³⁺ ions. The characteristic EPR spectrum of the Ni³⁺ (3d⁷) ions with $g_1 = 2.268$, $g_2 = 2.237$, and $g_3 = 2.045$ indicates that the Ni³⁺ ions are most likely located in the substitutional sites of TiO₂, possibly near the surface rutile phase. The Ni⁺ species (3d⁹) with $g_{||} = 2.130$ and $g_{\perp} = 2.063$ are on the surface of TiO₂. Both Ni⁺ and Ni³⁺ ions are quite stable in hydrogen. The Ni³⁺ ions seem to be responsible for anchoring the nickel ions onto titania and stabilizing the Ni⁺ species on the surface. The Ni⁺ ions are thus free from oxygen poisoning and still show a high activity toward olefin oligomerization.

INTRODUCTION

The Ni/TiO₂ catalytic system has been gaining considerable attention and research interest. Its exceptionally high activity along with higher hydrocarbon selectivity in the CO hydrogenation reactions has been reported due to an interaction between nickel and TiO₂.¹⁻³ Besides, the photogenerated Ni⁺ in Ni/TiO₂ showed potential in olefin oligomerization.⁴⁻⁵ It has been suggested that an interaction of a low valent nickel ion with an acid site would form active sites for olefin dimerization.⁶ The reducibility of TiO₂ led to a "strong metal-support interaction" (SMSI)⁷ state after a high temperature reduction of Ni/TiO₂ catalyst. The high reactivity of CO hydrogenation may not be due to the SMSI properties.⁸⁻¹⁰ It is therefore interesting to elucidate whether any of the non-zero valent metal ions exists in the interfaces of nickel and titania? Do these ions act as anchoring sites in the formation of nickel particles during further reduction?¹¹ A more decisive study of the generation as well as the stability of non-zero valent metal ions in the Ni/TiO₂ system is desirable. An EPR study of photoreduction of Ni/TiO₂ is then concerned.

In a previous paper,¹¹ we reported that Ni⁺ ions can be generated and stabilized on titania by either mild thermal reduction at 450 K or photoreduction in hydrogen at 77 K. The photoreduction is more effective in the formation of definite valence and coordination state of Ni⁺. In the present

paper, we examine the photoreduction of Ni/TiO₂ catalysts with various nickel contents. Other than the previous findings,¹¹ the Ni³⁺ ions were found not only to display characteristic structure properties but also to play important roles in the stabilization of Ni⁺ ions on the surface of the catalyst.

EXPERIMENTAL

Materials

Ni/TiO₂ samples with various Ni contents (0.1, 0.5 and 2 wt%) were prepared by an incipient wetness impregnation method as described previously.¹⁰ Nickel nitrate was manufacture of Ferak, Berlin. TiO₂ used was Degussa P-25 that consisted 85% anatase and 15% rutile with a surface area of ~50 m²/g.

Carbon monoxide and ethylene were obtained from Matheson Gas Products. Ethylene was used without further purification, while CO gas was allowed to pass through a molecular sieve (5A) to remove possible metal carbonyls. Hydrogen gas used was generated by a hydrogen generator (Mark V. L/Milton Roy, USA). High purity oxygen was supplied by San Fu Chemical Co..

Procedures

All samples were dried in a vacuum oven before being placed in an EPR cell. The EPR cell used is shown in Fig. 1.

It is designed with a quartz EPR tube on one end and a Pyrex reactor on the other end, so that the sample can be treated *in-situ* for the EPR measurements. Sparingly, to ensure a vacuum-tight system, the sample was first evacuated to about 10^{-5} torr at room temperature immediately after being placed in the cell. The sample was then oxidized in an oxygen flow at 773 K for two hours and finally evacuated at the same temperature for several hours before cooling to room temperature. Two hundred torrs of hydrogen were then introduced into the EPR cell. The photoreduction was performed at 77 K using a Rayonet Photochemical Reactor (model RPR-100) with RPR-2537 Å lamps, which gives a 253.7 nm UV source with an intensity of 1.65×10^{16} photons/cm²/sec.

Thermal treatment, degassing, and adsorption of gases was performed at room temperature with the EPR cell being attached to a greaseless, high-vacuum glass manifold.

The X-band EPR spectra were obtained by using a TE₁₀₂ rectangular cavity in a Bruker ER-200D EPR spectrometer. Most of the spectra were recorded at 77 K with

samples immersed in liquid nitrogen in a quartz dewar. The temperature dependence of EPR measurement was fulfilled with a Bruker ER-4111 VT variable temperature unit. Some spectra were taken at room temperature with the sample placed directly inside the standard EPR cavity. The *g* values of EPR signals were measured using a DPPH sample (*g* = 2.0036) as a reference.

RESULTS AND DISCUSSION

Photoreduction of Ni/TiO₂ and the EPR peak assignments

Fig. 2 shows the typical EPR spectra of the photoreduced Ni/TiO₂ catalysts in 200 torrs of hydrogen at 77 K. Each photoreduced catalyst had been warming up for a few seconds before the spectroscopic measurement. Spectra 2(a), (b), and (c) were obtained for the three Ni/TiO₂ catalysts with nickel contents of 0.1 wt%, 0.5 wt%, and 2.0 wt%, respectively. These spectra show that the relative quantum

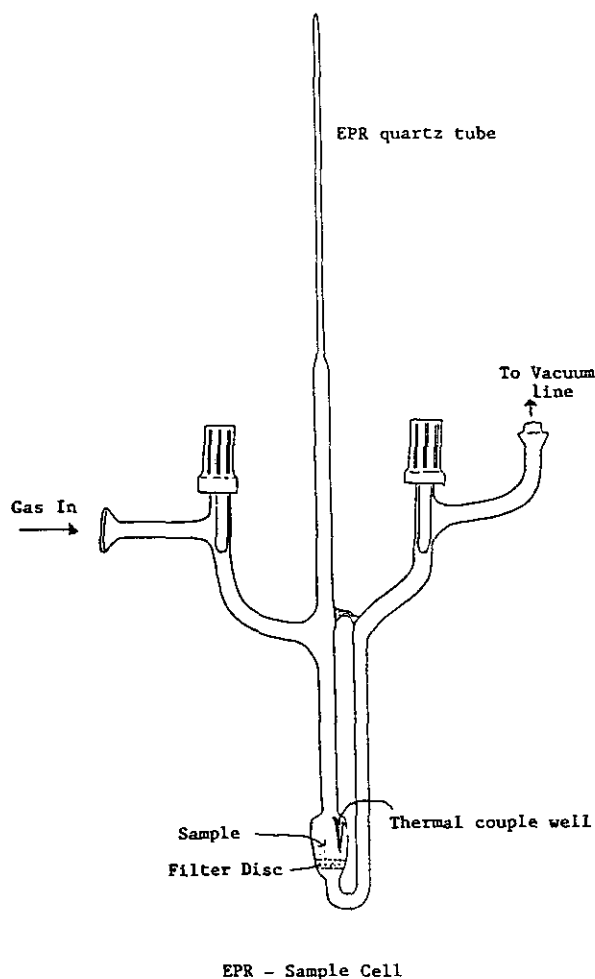


Fig. 1. The EPR cell used in this study.

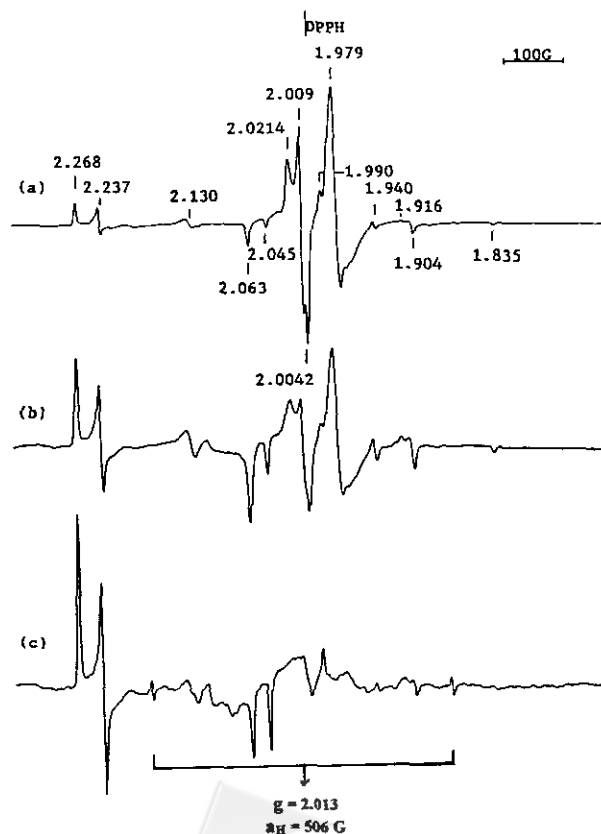


Fig. 2. EPR spectra of various Ni/TiO₂ catalysts after UV irradiation at 77 K in the presence of 200 torrs H₂. (a) 0.1 wt% Ni/TiO₂, (b) 0.5 wt% Ni/TiO₂, (c) 2.0 wt% Ni/TiO₂. All spectra were recorded at 77 K.

yields of the photogenerated paramagnetic species depend on the nickel content. In the present study, the quantum yield was not measured, since the efficiency of the photoreduction was found to be affected not only by the duration of the UV irradiation, but also by the purity of liquid nitrogen used during irradiation; condensation of oxygen or water in the liquid nitrogen trap caused a remarkable decrease in the efficiency of UV irradiation.

The EPR spectra shown in Fig. 2 are composed of several paramagnetic species. In order to describe the experimental results straightforwardly, the EPR peak assignments are briefly summarized as follows by comparison with the literature and the further experimental results. Further evidence and discussion of the peak assignments will be given later in this paper.

(1) The signal at $g_1 = 2.268$, $g_2 = 2.237$ and $g_3 = 2.045$ is assigned to the Ni³⁺ (3d⁷) in the substitutional sites of bulk TiO₂.¹²⁻¹³

(2) The signal at $g_{||} = 2.130$ and $g_{\perp} = 2.063$ is most likely due to Ni⁺ species (3d⁹).¹¹

(3) The relatively large signal appearing at $g_{\perp} = 1.979$ with a low field shoulder at $g = 1.990$, seen clearly in the 0.1 and 0.5 wt% of Ni/TiO₂ samples, is ascribed to Ti³⁺ (3d¹) located in bulk TiO₂.¹⁴⁻¹⁶

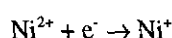
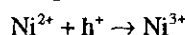
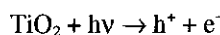
(4) The signal at $g_1 = 2.0214$, $g_2 = 2.0090$, and $g_3 = 2.0042$ is the typical EPR spectrum of O₂⁻.¹⁶⁻¹⁸

(5) The small signals at $g = 1.940$, 1.916, 1.904, and 1.835 might be caused either by the hyperfine or defect structure or the impurities in TiO₂; all these signals are also found in the bare Degussa P-25 TiO₂ sample after being out-gassed at 393 K.

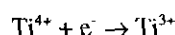
(6) The extra two tiny signals with their center appearing at $g = 2.013$ with a hyperfine coupling constant $a_H = 506$ Gauss as in Fig. 2(c) is due to the hydrogen atom.¹⁹ In some other experiments, the EPR signals due to the H atom were also detected in 0.1 and 0.5 wt% of Ni/TiO₂ for a shorter warming up period. It is quite certain that H atoms were generated during the UV irradiation. The H atom signal usually disappears when the sample is warmed up for a slightly longer time.

By taking the above peak assignment and comparing the relative spin concentration in the spectra as shown in Fig. 2, we observe that the less nickel was loaded in the sample, the weaker the Ni⁺ and Ni³⁺ peak intensities were, but the higher was the intensity of the Ti³⁺ peak. This might imply that, during the photoreduction of Ni/TiO₂ in H₂ at 77 K, the self-redox photoreaction of Ni²⁺ took place first, the reduction of Ti⁴⁺ to Ti³⁺ followed thereafter. The coexistence of Ni⁺ and Ni³⁺ species is considered due to the simultaneous oxidation and reduction of Ni²⁺ ions to form Ni³⁺ and

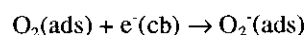
Ni⁺ species in the presence of TiO₂, which is a reducible oxide support and also a *n*-type semiconductor. Since the band gap of TiO₂ is about 3.02 eV,²⁰ UV irradiation will cause the formation of pairs of valence band holes (h⁺) and the conduction band electrons (e⁻). The Ni²⁺ ions might be partially oxidized by capturing the hole and partially reduced by the electron according to the following reactions:



The reduction may also be carried out by the electron due to the photogenerated hydrogen atom (H → H⁺ + e⁻). In the case of low nickel loading, the excess electrons are participating in the reduction of TiO₂:



The formation of O₂⁻(ads) species is most likely due to trapping of the adsorbed O₂ molecule onto the conduction band electron, e⁻(cb), according to the reaction:



In the present paper, we wish to report on the effect of TiO₂ supports on the stability of the unusual oxidation states of nickel ions, Ni⁺ and Ni³⁺; the study then focuses on the 2 wt% Ni/TiO₂ sample. Further studies on the EPR spectrum of the photogenerated Ti³⁺ ions in the TiO₂-supported metal (Ni, Rh and Pt) catalysts will be given in a separate paper.²¹

The EPR spectrum of Ni⁺ and Ni³⁺ in TiO₂

It has been shown that Ni⁺ ions can be stabilized on titania,¹¹ silica,²² alumina,²³ and zeolites.²⁴ Hydrogen and carbon monoxide are powerful probe molecules for detecting the existence of the monovalent Ni⁺ ions. With H₂ or CO as ligands, the complexes of Ni⁺ ions exhibit distinguished EPR signals. In the present study, the signal appearing at $g_{\perp} = 2.063$ is assigned to a Ni⁺ species in axial symmetry. This value is quite close to the reported values for the axial Ni⁺ species as in the photoreduced Ni/SiO₂.²³ From the spectra obtained after further reduction or oxidation treatments of the photoreduced Ni/TiO₂ samples, the variation of the peak intensity at $g = 2.130$ is almost linear with that at $g = 2.063$, the *g*-value of 2.130 is then assigned to the parallel *g*-component of Ni⁺ ion in the axial symmetry, although this value is quite far away from the reported data for silica- or alumina-supported nickel.²³

Ni^{3+} is a peculiar ion.¹² It has been reported to exist in nonstoichiometric NiO and to be responsible for the good performance of catalytic oxidation reactions.^{25,26} The existence of Ni^{3+} in the calcined Ni/TiO₂ has also been reported based on EXAFS and UV visible spectroscopic results.²⁷ Moreover, EPR spectra of two species of Ni^{3+} ions have been reported in the nickel-doped rutile TiO₂ (containing 0.01% nickel).^{12,13} One set of signals at $g_1 = 2.254$ and $g_1 = 2.084$ and 2.085 was assigned to the Ni^{3+} species occupying the interstitial sites of TiO₂. The other set of signals at $g_1 = 2.270$, $g_2 = 2.237$, and $g_3 = 2.050$ was suspected to be due to the Ni^{3+} in the substitutional site of TiO₂. The latter signal set appeared after the sample being illuminated and is thus called "light generated nickel". In our experiments of photoreduction of Ni/TiO₂ in hydrogen at 77 K, the EPR signal appearing at $g_1 = 2.268$, $g_2 = 2.237$, and $g_3 = 2.045$ is very closed to the latter signal set of the "light generated nickel" Ni^{3+} species in the substitutional sites of rutile TiO₂; the slight difference in g values was once suspected to be due to the anatase components in Degussa TiO₂ (~85% Anatase and ~15% Rutile). However, further experiments on Ni/rutile sample showed that the discrepancy is more likely ascribed to the difference between the thick crystal and the powder sample environments (see below).

The signals at $g_1 = 2.268$, $g_2 = 2.237$, and $g_3 = 2.045$ are then assigned to the Ni^{3+} ($3d^7$) in the substitutional sites of bulk TiO₂. The $g_3 = 2.045$ is the typical parallel component of an orthorhombic species; it follows roughly the intensity variation of the other two perpendicular components at $g = 2.268$ and 2.237 , as can be seen in all the spectra. The average g value of this paramagnetic species is thus 2.183, which is comparable with the reported g value of Ni^{3+} , for example $g = 2.1693$ for Ni^{3+} in MgO, 2.282 for Ni^{3+} in CaO, and 2.146 for Ni^{3+} in Al₂O₃.²⁸

In our experiments, no EPR spectrum of Ni^{2+} was detected at 77 K and only very small peak corresponding to the Ni^{3+} in the interstitial site was observed in a few cases.

To verify the Ni^{3+} EPR spectrum, we also carried out an experiment dealing with 2 wt% Ni sample supported on rutile-TiO₂. The sample was prepared by the incipient wetness impregnation method and rutile was obtained from Aldrich Co. Fig. 3(a) was obtained after the sample had been evacuated at 773 K. Sequential treatments include adding 200 torrs of hydrogen, UV irradiation in hydrogen at 77 K, and finally oxidation in oxygen at 773 K; the corresponding EPR spectra recorded at 77 K are shown in Figs. 3(b), (c), and (d), respectively. A slight difference in g -values as compared to those of the Degussa TiO₂-supported nickel is possible due to the nature of TiO₂.

The above results may indicate that Ni^{2+} ions tend to

occupy the substitutional sites of TiO₂ and subsequently oxidize to Ni^{3+} during the high temperature evacuation and low temperature UV irradiation. It is noticeable that the interstitial Ni^{3+} is observed only after the oxidation, especially oxidation at high temperature. The results are somewhat different from those reported in the literature,¹² that the normally observed Ni^{3+} spectrum occupies the interstitial position. Moreover, with rutile support, no monovalent state of nickel ion has been observed during UV irradiation of the sample in hydrogen at 77 K. This is not surprising, because rutile is photocatalytically less active than anatase²⁹ due to its small band gap energy.³⁰

The influence of the non-zero valent nickel ions (Ni^+ and Ni^{3+}) by hydrogen

To examine the stability of the Ni^+ and Ni^{3+} ions and their sensitivity to H₂ gas, sequential experiments were carried out on the 2 wt% Ni/TiO₂ catalyst. The results are

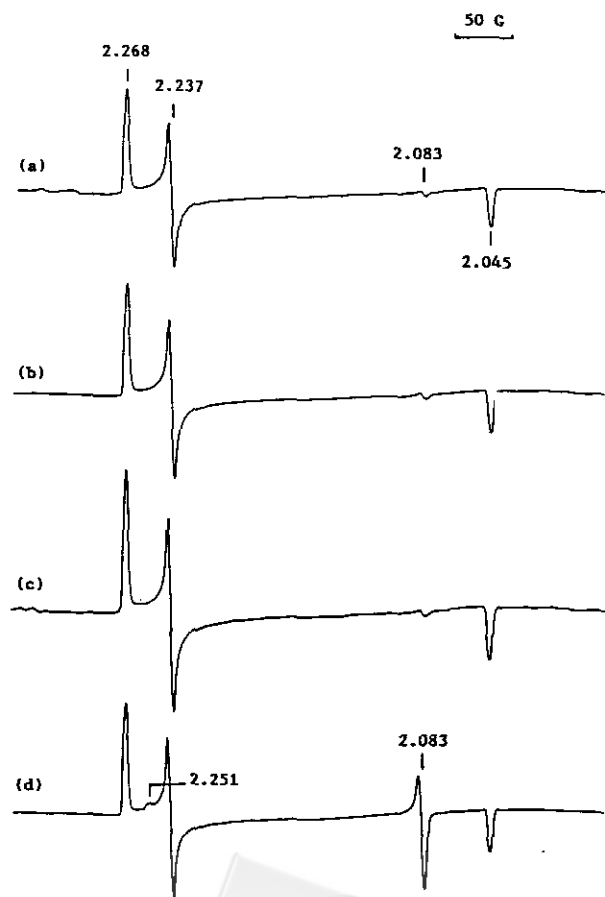


Fig. 3. EPR spectra of 2 wt% Ni/Rutile-TiO₂; spectra were recorded at 77 K after: (a) evacuation at 773 K, (b) addition of 200 torrs of hydrogen, (c) UV irradiation at 77 K for 2 hours, (d) oxidation and evacuation at 773 K.

shown in Fig. 4. Fig. 4(a) is the EPR spectra of the photoreduced sample that has been kept at room temperature for a certain time. By comparison with the spectrum of Fig. 2(c), there is no significant intensity change in the Ni³⁺ signal, but a remarkable decrease in the Ni³⁺ signal intensity; and the O₂⁻ signal appearing at $g = 2.0214, 2.0090$ and 2.0024 is clearly intensified. It might be possible that the Ni³⁺-O₂²⁻ complex had been formed in the photoreduced Ni/TiO₂ due to the ability of TiO₂ to stabilize O₂²⁻ species,³¹ as proposed by Espinós in the calcined Ni/TiO₂.²⁷ The changes in EPR peak intensities may be explained by the electron transfer between Ni³⁺ and O₂²⁻ leading to the formation of Ni²⁺ and O₂⁻. Consequently, there appeared a decrease in Ni³⁺, and an increase in O₂⁻.

A brief evacuation to 1×10^{-4} torr at room temperature resulted in a spectrum as shown in Fig. 4(b); further evacuation for 10 more minutes to a vacuum of 5×10^{-5} torr led to a spectrum as shown in Fig. 4(c). Readmission of 200 torrs of H₂, Fig. 4(d) was obtained. Figs. 4(e) and (f) are the results obtained by consecutive evacuation and addition of hydrogen. The signal intensities of g -value of 2.130 and 2.063 varies linearly and both are enhanced in the appearance of H₂. It is not clear whether the signal at $g_{\parallel} = 2.130$ and $g_{\perp} = 2.063$ is due to the reduced form (Ni²⁺), or the complex of Ni²⁺ with H₂ as ligands. However, according to its reversible formation and high sensitivity to the hydrogen, it is quite cer-

tain that the photogenerated paramagnetic Ni²⁺ species are in axial symmetry, located at the surface of the catalysts.

The spectra in Fig. 4 also show that Ni³⁺ EPR signals at $g = 2.268, 2.237, \text{ and } 2.045$ vary almost parallel in all the spectra, and gradually decrease during the subsequential treatments, but seem unaffected by the presence or absence of H₂. The Ni³⁺ species are in orthorhombic symmetry and most likely located in the framework of bulk TiO₂, but somehow near the surface as ascribed to the nature of the impregnated sample.

The influence of oxygen

The influence of O₂ on the photogenerated paramagnetic species is shown in Fig. 5. Fig. 5(a) is the EPR spectrum of 2 wt% Ni/TiO₂ in 200 torrs of hydrogen. The spectrum was recorded after Fig. 4(f). Fig. 5(b) was obtained when 200 torrs of O₂ were introduced to the outgassed sample. Apparently, the intensity due to Ni³⁺ at $g = 2.268, 2.237, \text{ and } 2.045$ is remarkably enhanced in the presence of O₂. In contrast, the Ni²⁺ signal ($g_{\perp} = 2.063, g_{\parallel} = 2.130$) disappeared, and the O₂⁻ signal ($g = 2.0214, 2.0090, \text{ and } 2.0042$) is completely quenched. There were no significant changes in the intensities of those small signals with g values less than 2.000. Evacuation of O₂ restored the Ni²⁺ signal, and enhanced the signal due to O₂⁻ species. The change in Ni³⁺ signal was somehow negligible. Again, this may indicate that the Ni³⁺ species are in the near-surface-bulk of TiO₂.

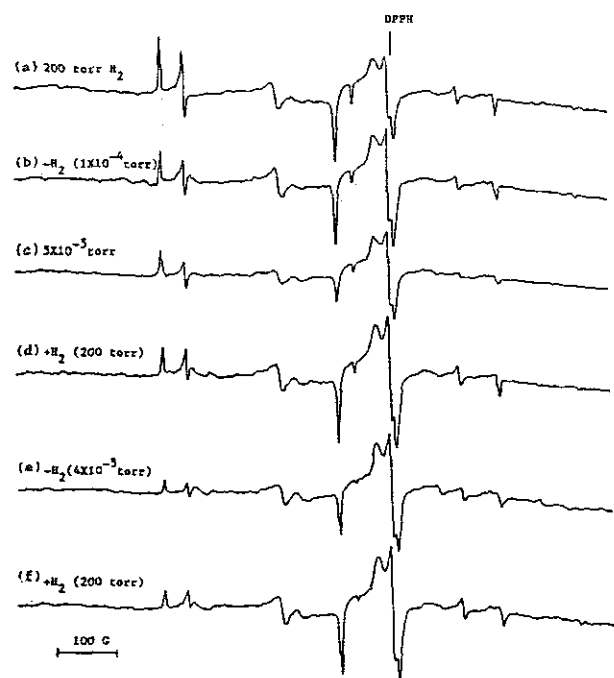


Fig. 4. Effect of hydrogen on the EPR spectra of the photoreduced 2 wt% Ni/TiO₂. All spectra were recorded at 77 K.

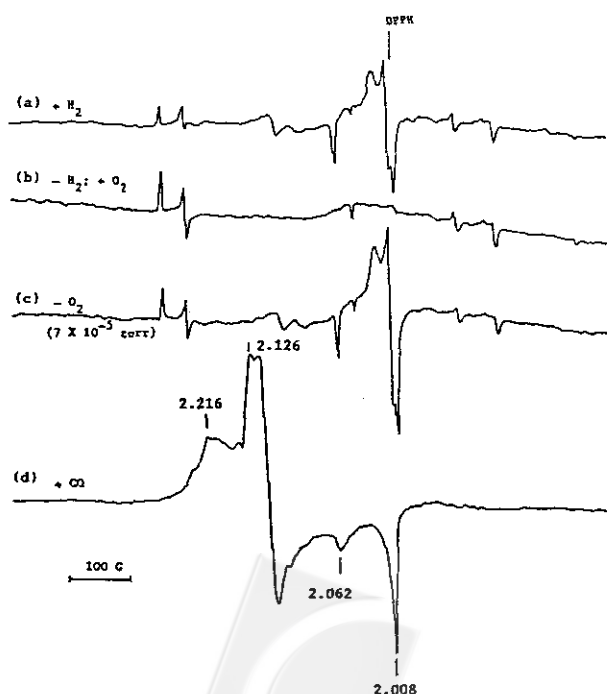


Fig. 5. Effect of oxygen on the stability of the paramagnetic species in the photoreduced 2 wt% Ni/TiO₂.

Fig. 5(d) was obtained when 200 torrs of carbon monoxide were introduced to the outgassed samples. It is essentially the same EPR spectrum of $\text{Ni}(\text{CO})_n^+$ discussed in the previous report¹¹ and in the literature.²³ The present results have exhibited that both surface Ni^+ species and bulk Ni^{3+} ions are quite stable in the photoreduced Ni/TiO_2 catalysts, whether exposed to H_2 or O_2 at room temperature.

Temperature dependent EPR spectrum

Fig. 6 shows the temperature dependence of EPR spectra of 2 wt% Ni/TiO_2 in hydrogen after UV irradiation at 77 K. The signal intensities of Ni^+ and Ni^{3+} ions decreased as

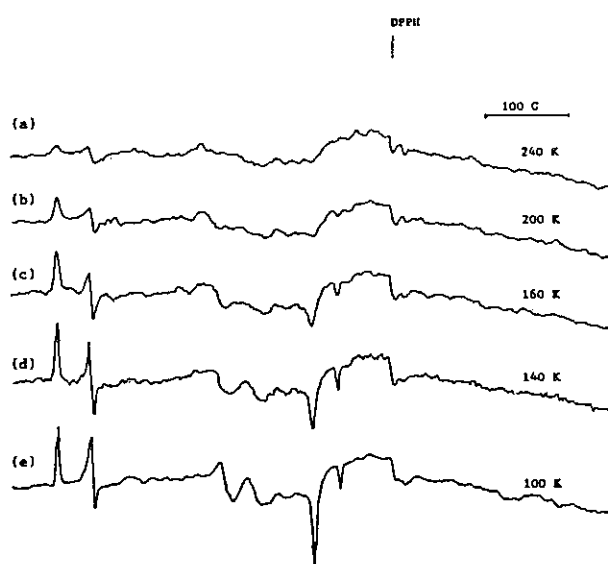


Fig. 6. Temperature dependence of EPR spectrum of the photoreduced 2 wt% Ni/TiO_2 .

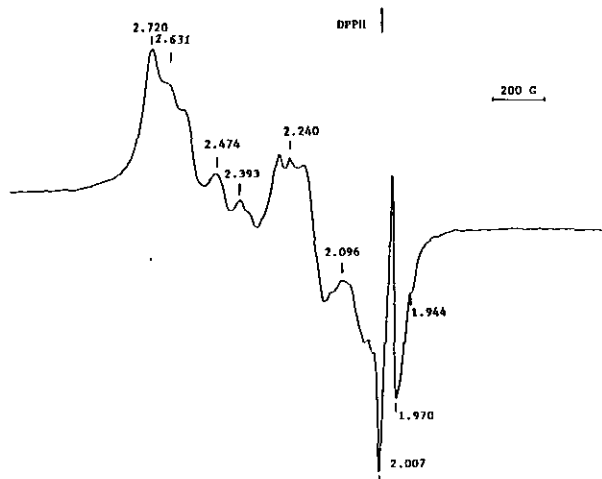


Fig. 7. EPR spectrum of photoreduced 2 wt% Ni/TiO_2 in 200 torrs of ethylene.

the recording temperature increased. The signals of Ni^+ ions are beyond detection around 200 K, while the Ni^{3+} signals were traceable up to 240 K. For those with g values less than 2.00 ($g = 1.941, 1.904, \text{ and } 1.832$), signals did not appear above 100 K. It is still hard to tell whether these signals are due to the hyperfine structure of Ti^{3+} , or the defect structure of TiO_2 , or other impurities in the Degussa P-25 TiO_2 .

Olefin oligomerization

It had been reported that the coordinately unsaturated Ni^+ ions on the surface of silica or alumina, or in zeolite X are very active at room temperature in ethylene and propylene oligomerization.^{4,5,31,32} It is found that the photoreduced Ni/TiO_2 sample also shows considerably high catalytic activity in ethylene oligomerization. 200 torrs of ethylene were admitted to the outgassed photoreduced Ni/TiO_2 samples at room temperature and then immersed in the liquid nitrogen. The EPR spectrum as shown in Fig. 7 was recorded at 77 K. By comparison with data in the literature,^{4,5} the complicated spectrum shows the superimposed spectra due to hexene, butene, propene, and ethylene, although they are not quite resolved.

CONCLUSION

UV irradiations of Ni/TiO_2 in H_2 at 77 K produced Ni^+ , Ni^{3+} , and Ti^{3+} ions. The present EPR spectroscopic study has elucidated the characteristic structure, stability, and catalytic properties of the photogenerated species. It was found that photoreduction of Ti^{4+} to Ti^{3+} showed less priority than the self-redox photoreactions of Ni^{2+} ions to form Ni^+ and Ni^{3+} ions. The Ni^{3+} ions are in orthorhombic symmetry and located in the substitutional site of TiO_2 in the interface or near the surface rutile phase. The formation of nickel-peroxy species ($\text{Ni}^{3+}-\text{O}_2^{\cdot-}$) might also be possible in the photoreduced Ni/TiO_2 . The Ni^{3+} ions seem to be responsible for anchoring the nickel ions onto titania and stabilizing the Ni^+ species on the surface. The Ni^+ species are in axial symmetry located at the surface of the catalyst. They are highly stable in hydrogen, oxygen, and CO and are active for olefin oligomerization.

ACKNOWLEDGMENT

We gratefully acknowledge the financial support from the National Science Council, Republic of China.

Received December 31, 1996.

Key Words

EPR spectrum; Ni⁺; Ni³⁺; TiO₂.

REFERENCES

1. Vannice, M. A.; Garten, R. L. J. *J. Catal.* **1979**, *56*, 236; **1980**, *66*, 242.
2. Burch, R.; Flambard, A. R. *J. Catal.* **1982**, *78*, 389; *J. Chem. Soc. Chem. Comm.* **1981**, 123; *Stud. Surf. Sci. Catal.* **1982**, *11*, 193.
3. Turlier, P.; Martin, G. A. *React. Kinet. Catal. Lett.* **1982**, *19*, 275; **1982**, *21*, 387; *Stud. Surf. Sci. Catal.* **1982**, *11*, 203.
4. Kazansky, V. B.; Elev, I. V.; Shelimov, B. N. *J. Mol. Catal.* **1983**, *21*, 265.
5. Bonneviot, L.; Olivier, D.; Che, M. *J. Mol. Catal.* **1983**, *21*, 415.
6. Kimura, K.; Ozaki, A. *J. Catal.* **1970**, *18*, 271.
7. Tauster, S. J.; Fung, S. C.; Garten, R. L. *J. Amer. Chem. Soc.* **1978**, *100*, 170.
8. Fang, S. H.; White, J. M.; Campione, T. J.; Ekerdt, J. G. *J. Catal.* **1985**, *96*, 491.
9. Sohn, J. R.; Kim, H. J. *J. Catal.* **1986**, *102*, 428.
10. Chien, S. H.; Chang, Y. C. *Bull. Inst. Chem., Academia Sinica* **1989**, *36*, 81.
11. Chien, S. H.; Shao, L. Y.; Che, M.; Bonneviot, L. *Solid State Ionics* **1989**, *32/33*, 962.
12. Gerritsen, H. J.; Sabisky, E. S. *Phys. Rev.* **1962**, *125*, 1853.
13. Gerritsen, H. J. in *Paramagnetic Resonance*, vol. 1, ed. W. Low, Academic Press, New York, **1963**, p 3.
14. Bonneviot, L.; Haller, G. L. *J. Catal.* **1988**, *113*, 96.
15. Conesa, J. C.; Soria, J. *J. Phys. Chem.* **1982**, *86*, 1392.
16. Tuel, A.; Diab, J.; Gelin, P.; Dufaux, M.; Dutel, J-F.; Taarit, Y. B. *J. Mol. Catal.* **1990**, *63*, 95.
17. Howe, R. F.; Grätel, M. *J. Phys. Chem.* **1987**, *91*, 3906.
18. Lunsford, J. H. *Catal. Rev.* **1973**, *8*, 135.
19. Cole, T.; Silver, A. H. *Nature* **1963**, *200*, 700.
20. Borgarello, E.; Serpone, N.; Emo, G.; Harris, R.; Pelizzatti, E.; Minero, C. *Inorg. Chem.* **1986**, *25*, 4499.
21. Chien, S. H.; Chen, B. C.; Lin, M. C. to be published.
22. Bonneviot, L.; Olivier, D.; Che, M. *J. Chem. Soc., Chem. Commun.* **1982**, 952.
23. Bonneviot, L.; Che, M.; Dyrek, K.; Schöllner, R.; Wendt, G. *J. Phys. Chem.* **1986**, *90*, 2379, and the references therein.
24. Kermarrec, M.; Olivier, D.; Richard, M.; Che, M.; Bazon-Verduraz, F. *J. Phys. Chem.* **1982**, *86*, 2818.
25. Badyal, J. P.; Zhang, X.; Lambert, R. M. *Surf. Sci.* **1990**, *225*, L15.
26. Gravelle, P. C.; Teichner, S. J. in *Advances in Catalysis*, eds. D. D. Eley, H. Pines and P. B. Weisz, Vol. 20, Academic Press, New York, **1969**, p 167.
27. Espinós, J. P.; González-Eliphe, A. R.; Caballero, A.; García, J.; Munuera, G. *J. Catal.* **1992**, *136*, 415.
28. Abragam, A.; Bleaney, B. in *Electron Paramagnetic Resonance of Transition ions*, Dover Pub., **1986**, p 487.
29. Brown, J. D.; Williamson, D. L.; Nozik, A. J. *J. Phys. Chem.* **1985**, *89*, 3706.
30. Schindler, K.-M.; Kunst, M. *J. Phys. Chem.* **1990**, *94*, 8222.
31. Munuera, G.; González-Eliphe, A. R.; Fernández, A.; Malet, P.; Espinós, J. P. *J. Chem. Soc. Faraday Trans. 1*, **1989**, *85*, 1279.

